

000 001 002 003 004 005 006 007 008 009 010 011 012 013 014 015 016 017 018 019 020 021 022 023 024 025 026 027 028 029 030 GRAPH SYNTHETIC OUT-OF-DISTRIBUTION EXPOSURE WITH LARGE LANGUAGE MODELS

005 **Anonymous authors**

006 Paper under double-blind review

009 ABSTRACT

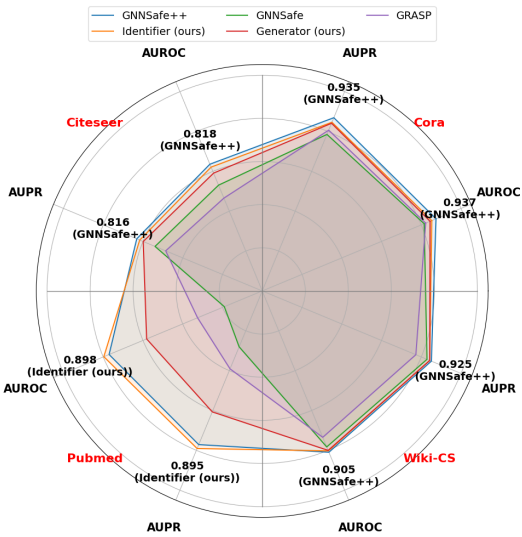
012 Out-of-distribution (OOD) detection in graphs is critical for ensuring model ro-
013 bustness in open-world and safety-sensitive applications. Existing graph OOD
014 detection approaches typically train an in-distribution (ID) classifier on ID data
015 alone, then apply post-hoc scoring to detect OOD instances. While *OOD expo-*
016 *sure*—adding auxiliary OOD samples during training—can improve detection,
017 current graph-based methods often assume access to real OOD nodes, which is
018 often impractical or costly. In this paper, we present GOE-LLM, a framework
019 that leverages Large Language Models (LLMs) to achieve OOD exposure on text-
020 attributed graphs without using any real OOD nodes. GOE-LLM introduces two
021 pipelines: (1) identifying pseudo-OOD nodes from the initially unlabeled graph
022 using zero-shot LLM annotations, and (2) generating semantically informative
023 synthetic OOD nodes via LLM-prompted text generation. These pseudo-OOD
024 nodes are then used to regularize ID classifier training and enhance OOD detection
025 awareness. Empirical results on multiple benchmarks show that GOE-LLM sub-
026 stantially outperforms state-of-the-art methods without OOD exposure, achieving
027 up to a 23.5% improvement in AUROC for OOD detection, and attains performance
028 on par with those relying on real OOD nodes for exposure.

029 1 INTRODUCTION

031 Graph data is widely used to model interactions among entities in social networks, citation networks,
032 transaction networks, recommendation systems, and biological networks Xiao et al. (2020); Zhu et al.
033 (2022); Xu et al. (2021; 2020); Lee et al. (2020). In many practical scenarios, nodes are paired with
034 rich textual attributes—such as user bios, paper abstracts, or product descriptions—leading to *text-*
035 *attributed graphs* (TAGs) Yang et al. (2021); Yan et al. (2023). These graphs integrate both structural
036 and semantic information, enabling more fine-grained learning and inference tasks. Recently, *out-*
037 *of-distribution (OOD) detection* on graphs Wu et al. (2023); Ma et al.; Xu et al. (2025b); Zhao et al.
038 (2020); Xu et al. (2025a); Wang et al. (2025); Xu et al. (2025b) has become increasingly studied
039 for safety-critical and open-world applications. The goal is to identify nodes whose distribution
040 significantly deviates from the in-distribution (ID) training classes. This task is particularly relevant
041 in real-world applications where unseen or anomalous entities may appear during inference—such as
042 emerging users in social platforms and new research domains in citation graphs.

043 **OOD Exposure and Its Applicability to Graphs.** Most existing graph OOD detection methods
044 adopt a semi-supervised, transductive setup in which all nodes are accessible during training, but
045 only a subset of classes is labeled Ma et al.; Song & Wang (2022); Xu et al. (2025a). Training solely
046 on ID data can lead to overconfident predictions on OOD nodes Inkawich et al. (2021), making
047 subsequent post-hoc OOD scoring less reliable. It can be even worse if OOD instances are structurally
048 or semantically similar to ID data. A widely-used strategy for mitigating this overconfidence is
049 *OOD exposure*, wherein additional OOD samples are incorporated during training Hendrycks et al.
050 (2022; 2018); Zhang et al. (2023); Du et al. (2024). However, existing approaches often rely on real
051 OOD labels—an assumption that is unrealistic in many graph settings Wu et al. (2023), where OOD
052 nodes are elusive or costly to label. In other domains (images, text), recent work has investigated
053 generating *pseudo-OOD* instances Tao et al. (2023); Abbas et al. (2025); Cao et al. (2024); Du et al.
Models (LLMs) have been used to create OOD proxies for text detection Abbas et al. (2025) or

054 outlier exposure Cao et al. (2024), yet these techniques are not directly applicable to graph data due
 055 to the complexity of node interconnections.
 056



074 Figure 1: Our graph OOD detection method does
 075 not rely on any real OOD nodes for training, yet
 076 achieves significantly better OOD detection perfor-
 077 mance than baseline methods and performs com-
 078 parably to the approach that uses real OOD nodes
 079 (GNNSafe++) for exposure.

080 In practice, GOE-*identifier* is convenient when a graph already provides sufficient semantic
 081 context, allowing the LLM to reliably mark OOD nodes from unlabeled data. By contrast,
 082 GOE-*generator* is preferable if node text is limited or if broad OOD concepts must be introduced.
 083 It also applies naturally in inductive scenarios where future nodes—unseen at training time—may be
 084 OOD. Meanwhile, GOE-*identifier* targets a transductive setting, since potential OOD nodes
 085 must exist beforehand. Overall, GOE-*identifier* provides a lightweight way to detect OOD
 086 within the given graph, whereas GOE-*generator* synthesizes new OOD samples when no suitable
 087 OOD data or domain knowledge is available in the unlabeled set.

088 We summarize our key contributions as follow:

- **First Method for LLM-Powered Graph OOD Exposure.** We present a new approach to graph OOD detection with exposure that does not need real OOD labels, leveraging LLMs for pseudo-OOD identification and generation.
- **Exploration of LLM Roles in OOD Exposure.** We propose two approaches for pseudo-OOD supervision: using an LLM as a pseudo-OOD node *identifier* and as a pseudo-OOD node *generator*. GOE-*identifier* is effective in the transductive setting with rich unlabeled node semantics and requires no prior OOD knowledge. GOE-*generator* is applicable to the inductive setting and can introduce novel OOD concepts, but it benefits from a global understanding of OOD semantics.
- **Effectiveness.** Experimental results demonstrate that our method significantly outperforms baselines without OOD exposure and performs similarly to methods that use real OOD nodes for exposure. The code is available at: https://anonymous.4open.science/r/GOE_LLM-05B7/README.md.

102 2 RELATED WORK

103 2.1 GRAPH OOD DETECTION

105 Detecting OOD samples has been extensively investigated in the graph domain. GNNSafe Wu
 106 et al. (2023) reveals that standard GNN classifiers inherently exhibit some ability to distinguish
 107 OOD nodes, and it proposes an energy-based discriminator trained with a standard classification
 objective. OODGAT Song & Wang (2022) introduces a feature-propagation mechanism that explicitly

Our Proposal: GOE-*identifier* and GOE-*generator*. In this paper, we address OOD detection on TAGs by leveraging LLMs to generate OOD supervision signals without using real OOD samples. Specifically, we design two pipelines that inject pseudo-OOD information into training: First: GOE-*identifier*. We randomly sample a small set of unlabeled nodes and prompt an LLM for zero-shot OOD detection. If the LLM concludes that a node does not match any known ID classes, it labels that node as “none,” effectively designating it OOD. Despite potential label noise, these *identified* OOD nodes are then used as auxiliary training data to regularize the ID classifier. Second: GOE-*generator*. Instead of annotating existing nodes, we instruct the LLM to *generate* new pseudo-OOD nodes. These are inserted into the original graph to provide OOD signals during regularization training, enhancing the ID classifier’s ability to separate OOD from ID classes. Fig. 1 shows that both strategies outperform baselines w/o OOD exposure, while matching approaches with real OOD data.

GOE-*identifier* vs. GOE-*generator*.

108 separates inliers from outliers, unifying node classification and outlier detection in a single framework.
 109 GRASP Ma et al. demonstrates the benefit of OOD score propagation and theoretical guarantees for
 110 post-hoc node-level OOD detection, supplemented by an edge-augmentation strategy. More recently,
 111 GNNSafe++ Wu et al. (2023) extends GNNSafe by leveraging real OOD node labels for outlier
 112 exposure via an auxiliary regularization objective. However, methods that rely on actual OOD node
 113 labels are costly or infeasible, as identifying representative OOD nodes in graphs is non-trivial. Our
 114 work addresses the need for OOD exposure *without* real OOD data, specifically on TAGs.

115 2.2 OOD DETECTION WITH OOD EXPOSURE

117 A common strategy to mitigate overconfidence in neural networks is *OOD exposure*, which incor-
 118 porates OOD examples during training Hendrycks et al. (2018); Yang et al. (2024). In image-based
 119 setups, several methods rely on real OOD samples or external datasets, sometimes using mixing
 120 strategies to expand the OOD coverage Hendrycks et al. (2022); Zhang et al. (2023). For instance,
 121 OECC Papadopoulos et al. (2021) appends a confidence-calibration term to further separate ID
 122 and OOD regions, and MixOE Zhang et al. (2023) systematically mixes ID samples with known
 123 outliers to smooth the decision boundary. However, such techniques are limited by the availability
 124 and quality of genuine OOD data Du et al. (2024), which can be difficult or expensive to acquire in
 125 practice—particularly for graph data.

126 **Pseudo-OOD Generation.** To circumvent the requirement for real OOD examples, recent efforts
 127 have explored *pseudo-OOD generation*. VOS Du et al. (2022) synthesizes OOD representations from
 128 within the model’s latent space, and Vernekar et al. (2019) proposes a method to train an $(n+1)$ -class
 129 classifier by generating OOD samples in the image domain. Likewise, EOE Cao et al. (2024) uses
 130 LLMs to envision outlier concepts for image-based OOD detection, while Abbas et al. (2025) uses
 131 LLMs to create high-quality textual proxies for text OOD detection. Despite their successes, these
 132 approaches typically overlook graph-specific challenges, where node connectivity and structural
 133 information must be modeled alongside semantic content. Indeed, image and text instances are mostly
 134 independent, but graph nodes have relational dependencies among neighbors, making it non-trivial
 135 to adapt existing pseudo-OOD methods to the graph domain. In this paper, we focus on TAGs and
 136 propose using LLMs to identify and generate OOD nodes without relying on any real OOD data,
 137 bridging the gap left by prior work that has concentrated on images, text, or real OOD nodes in
 graphs. A detailed comparison of the above methods is presented in Appendix K.

138 3 METHODOLOGY

140 Here, we introduce GOE-LLM, a framework that integrates pseudo-OOD exposure into TAG learning
 141 without requiring real OOD nodes. Fig. 2 summarizes the overall pipeline. Section 3.2 describes
 142 the general process of graph OOD exposure, which uses real or pseudo-OOD nodes to regularize
 143 the training of the ID classifier. Sections 3.3 and 3.4 detail our proposed methods for graph OOD
 144 exposure without real OOD nodes: using an LLM as an OOD node identifier and as an OOD node
 145 generator, respectively. Finally, Section 3.5 discusses additional strategies for training a synthetic
 146 OOD model to incorporate OOD information into the ID classifier.

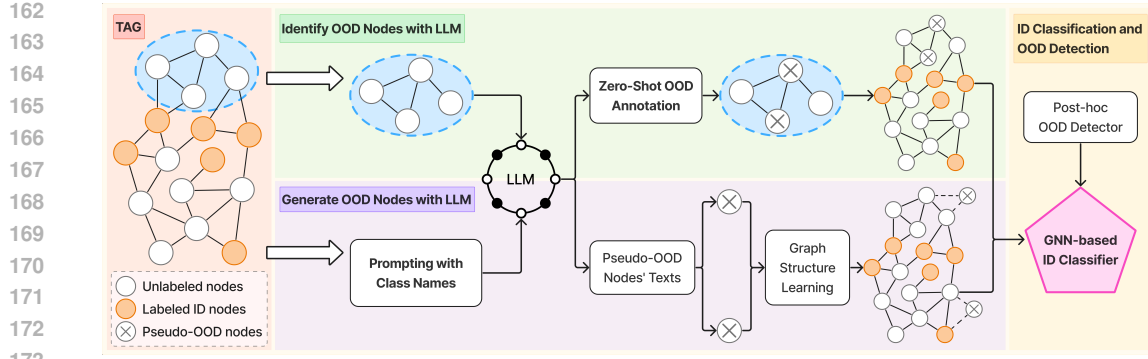
147 3.1 PRELIMINARIES

149 We study node-level OOD detection in TAGs, represented as $G_T = (\mathcal{V}, \mathbf{A}, \mathbf{T}, \mathbf{X})$, where $\mathcal{V} =$
 150 $\{v_1, \dots, v_n\}$ is the node set with textual attributes $\mathbf{T} = \{t_1, \dots, t_n\}$. Text embeddings $\mathbf{X} =$
 151 $\{x_1, \dots, x_n\}$ are derived from \mathbf{T} (e.g., via SentenceBERT Reimers (2019)), and $\mathbf{A} \in \{0, 1\}^{n \times n}$ is
 152 the adjacency matrix with $\mathbf{A}[i, j] = 1$ if v_i and v_j are connected.

153 **Node-level Graph OOD Detection.** We split the nodes into a labeled set \mathcal{V}_I (ID nodes) and an
 154 unlabeled set \mathcal{V}_U , with $\mathcal{V}_I \cap \mathcal{V}_U = \emptyset$ and $\mathcal{V}_I \cup \mathcal{V}_U = \mathcal{V}$. Each labeled node belongs to one of
 155 K known ID classes $\mathcal{Y}_I = \{y_1, \dots, y_K\}$. Unlabeled nodes may be either ID or OOD (i.e., from
 156 unknown classes not in \mathcal{Y}_I). We adopt a semi-supervised, transductive setting: the entire graph is
 157 observable at training time, but only \mathcal{V}_I is labeled. The goal is to decide, for each $v_i \in \mathcal{V}_U$, whether
 158 it belongs to one of the ID classes or is OOD.

159 3.2 GRAPH OOD DETECTION WITH PSEUDO-OOD EXPOSURE

160 **ID Classifier.** OOD exposure incorporates OOD-like samples during training to tighten the boundary
 161 around ID data. We first train a two-layer GCN classifier using only ID-labeled nodes (\mathcal{V}_I):



$$\mathcal{L}_{\text{sup}} = -\frac{1}{|\mathcal{V}_I|} \sum_{i \in \mathcal{V}_I} \sum_{k=1}^K y_{ik} \log \hat{y}_{ik}, \quad (1)$$

where \hat{y}_{ik} is the predicted probability that node v_i belongs to class k . After training, any post-hoc OOD scoring function can be applied. One common choice is the negative energy score Liu et al. (2020), where the OOD score for a node v_i with logits $z_i \in \mathbb{R}^K$ is

$$S_{\text{OOD}}(v_i) = -E(v_i) = \log \sum_{k=1}^K \exp(z_{ik}). \quad (2)$$

A larger $S_{\text{OOD}}(v_i)$ indicates that v_i is more likely OOD.

Pseudo-OOD Exposure. To refine the boundary between ID and OOD, we augment the training set with a set \mathcal{V}_O of OOD-like nodes. We then introduce a regularization term $\mathcal{L}_{\text{expo}}$ that enforces contrasting OOD scores for ID nodes and OOD nodes. Specifically, we penalize ID nodes whose OOD scores exceed a margin s_{id} and OOD nodes whose OOD scores fall below a margin s_{ood} . The overall loss is $\mathcal{L}_{\text{sup}} + \lambda \mathcal{L}_{\text{expo}}$, where λ balances ID classification accuracy and OOD discriminability.

$$\mathcal{L}_{\text{expo}} = \frac{1}{|\mathcal{V}_I|} \sum_{v_i \in \mathcal{V}_I} (\text{ReLU}(S_{\text{OOD}}(v_i) - s_{\text{id}}))^2 + \frac{1}{|\mathcal{V}_O|} \sum_{v_j \in \mathcal{V}_O} (\text{ReLU}(s_{\text{ood}} - S_{\text{OOD}}(v_j)))^2 \quad (3)$$

where s_{id} and s_{ood} are margin parameters, and \mathcal{V}_O can consist of either human-annotated OOD nodes or synthetic ones derived from LLMs.

3.3 IDENTIFY OOD NODES WITH LLMs

In this setting, rather than relying on real OOD nodes to train the ID classifier, we assume a more challenging and realistic scenario where there is no access to any OOD nodes or even the names of OOD classes. To address this, we leverage the transductive nature of graph learning and propose a novel approach that instructs LLMs to identify potential OOD nodes directly from the original graph. The identified pseudo-OOD nodes are then used to regularize the training of the ID classifier. Specifically, we first randomly sample a small set of nodes $\mathcal{V}_U^{\text{sampled}}$ from \mathcal{V}_U and let the LLM annotate them. The LLM is only provided with ID knowledge (ID class names) and prompted to determine whether the unlabeled query node belongs to an ID class, using its textual information. We instruct the LLM to output "none" if it determines that the node does not belong to any predefined ID class.

216 After that, we select the nodes identified by the LLM as OOD to form the pseudo-OOD node set \mathcal{V}_O ,
 217 as shown in Eqn. 4. Using this annotated set \mathcal{V}_O , we then train the ID classifier with Eqn. 3.
 218

$$219 \quad \mathcal{V}_O = \{v \in \mathcal{V}_U^{\text{sampled}} \mid \text{LLM}(\text{prompt}(v, \mathcal{C}_{\text{id}})) = \text{"none"}\} \quad (4)$$

220 where \mathcal{C}_{id} denotes the set of ID category names.
 221

222 3.4 GENERATE OOD NODES WITH LLMs

223 Instead of using LLMs to identify potential OOD nodes in the graph, we propose an alternative
 224 approach that leverages LLMs to generate pseudo-OOD nodes and insert them into the original graph
 225 for OOD supervision. These generated nodes constitute the OOD instances \mathcal{V}_O as defined in Eqn. 3.
 226 In this setting, we assume access only to the label names of all classes, without any real OOD nodes.
 227 For each OOD class, we use the LLM to generate M samples, leveraging its inherent large-scale
 228 knowledge of the respective class domains. The resulting text descriptions of the pseudo-OOD nodes
 229 are denoted by \mathbf{T}^{ood} , and the generation process is formalized in Eqn. 5.
 230

$$231 \quad \mathcal{V}_O = \{v_m^{\text{ood}} \mid \mathbf{T}_m^{\text{ood}} = \text{LLM}(\text{prompt}(c)), 1 \leq m \leq M, c \in \mathcal{C}_{\text{ood}}\} \quad (5)$$

232 where \mathcal{C}_{ood} denotes the set of OOD category names. By applying SentenceBERT Reimers (2019)
 233 to \mathbf{T}^{ood} , we obtain the embeddings of the pseudo-OOD nodes as \mathbf{X}^{ood} . The complete set of node
 234 embeddings is then given by $\mathbf{X}_{\text{aug}} = \mathbf{X} \parallel \mathbf{X}^{\text{ood}}$. Optionally, with graph structure learning, we can
 235 incorporate the pseudo-OOD nodes into the original graph to better propagate information through
 236 the new graph structure, denoted as \mathbf{A}_{aug} . One way to construct \mathbf{A}_{aug} is by creating edges based on
 237 the similarity of node embeddings. Alternatively, a negative sampling-based link prediction task can
 238 be performed to infer potential links. Using \mathbf{X}_{aug} and \mathbf{A}_{aug} , we then train the ID classifier on the
 239 augmented graph. This approach reframes OOD detection as an active and generative strategy—rather
 240 than a passive inference task—by leveraging textual priors to construct meaningful semantic contrast
 241 without requiring real OOD data.
 242

243 3.5 SYNTHETIC OOD MODEL

244 Thus far, we have proposed using pseudo-OOD nodes to regularize the training of a K -class ID
 245 classifier and applying post-hoc OOD detectors on top of the well-trained ID classifier for OOD
 246 detection. The main advantage of this approach is that it does not require modifying the network
 247 architecture of the ID classifier. However, it introduces a trade-off weight λ in the loss function.
 248 Intuitively, if λ is too large, it may degrade ID classification performance. Conversely, if λ is too
 249 small, the OOD information may not be sufficiently exposed to the ID classifier to improve its OOD
 250 awareness. To address this, we provide two alternative approaches that leverage both labeled ID
 251 nodes and synthetic noisy OOD nodes to train a model with enhanced OOD awareness.
 252

253 The first approach involves adding a binary classification layer on top of the standard ID classifier
 254 trained using Eqn. 1 to predict OOD scores. Specifically, we first train the ID classifier using labeled
 255 ID nodes. Once trained, we freeze the ID classifier and fit the weights of the binary OOD detector
 256 using a small set of labeled ID nodes along with the pseudo-OOD samples. The key advantage of
 257 this method is that it preserves the ID predictions of the pre-trained classifier while equipping the
 258 model with the capability to detect OOD nodes through the additional binary layer. The second
 259 approach extends the ID classifier into a $(K + 1)$ -way classification model, where the first K classes
 260 correspond to the ID classes and the $(K + 1)$ -th class represents the OOD class. The model is trained
 261 using both labeled ID nodes and pseudo-OOD nodes under a unified cross-entropy loss. The primary
 262 advantage of this joint classification approach lies in its flexibility to simultaneously learn accurate ID
 263 predictions while distinguishing between ID and OOD nodes, thereby enhancing overall performance.
 264

265 4 EXPERIMENTS

266 4.1 EXPERIMENTAL SETUP

267 **Datasets** We utilize the following TAG datasets, which are commonly used for node classification:
 268 Cora McCallum et al. (2000), Citeseer Giles et al. (1998), Pubmed Sen et al. (2008) and Wiki-CS
 269 Mernyei & Cangea (2020). The dataset descriptions are in Appendix B. We follow previous work
 270 Song & Wang (2022) by splitting the node classes into ID and OOD classes, ensuring that the number
 271 of ID classes is at least two to support the ID classification task. The specific class splits and ID ratios
 272 are detailed in Appendix A.
 273

270 **Training and Evaluation Splits** For each dataset with K ID classes, we use $20 \times K$ of ID nodes for
 271 training. Additionally, we randomly select $10 \times K$ of ID nodes along with an equal number of OOD
 272 nodes for validation. The test set consists of 500 randomly selected ID nodes and 500 OOD nodes.
 273 All experiments are repeated with five random seeds, and results are averaged.

274 **Baselines** We compare GOE-LLM with baselines: (1) **MSP** Hendrycks & Gimpel (2016), (2)
 275 **Entropy**, (3) **Energy** Liu et al. (2020), (4) **GNNSafe** Wu et al. (2023), and (5) **GRASP** Ma et al., all
 276 of which are post-hoc OOD detection methods without exposure. We also include **OE** Hendrycks
 277 et al. (2018) and **GNNSafe++** Wu et al. (2023), which leverage real OOD samples for exposure.
 278

279 **LLM-Powered OOD Exposure.** We use GPT-4o-mini for pseudo-OOD identification and generation.
 280 For node identification, we randomly sample 200 unlabeled nodes per dataset and prompt the LLM
 281 to classify them as either ID or OOD. Nodes predicted as OOD are used as pseudo-OOD exposure
 282 data. For pseudo-OOD generation, we prompt the LLM to generate $10 \times K_{\text{ood}}$ nodes, where K_{ood}
 283 denotes the number of OOD classes. The generated node texts are embedded using SentenceBERT
 284 Reimers (2019), and the resulting embeddings are concatenated with the original graph embeddings.
 285 We leave the exploration of more advanced graph structure learning methods for constructing the
 286 augmented graph to future work. Details on the efficiency of our method are provided in Appendix F.
 287

288 **Implementation details** For fair comparison, all ID classifiers are implemented using 2-layer GCNs
 289 with hidden dimension 32. We use Adam optimizer with learning rate 0.01, dropout rate 0.5, and
 290 weight decay of 5e-4. For all OOD exposure methods, the trade-off weight λ in the loss function
 291 is selected from {0.01, 0.05} based on the results of the validation set. For all methods, we set the
 292 maximum number of training epochs to 200 and apply early stopping if the sum of AUROC and ID
 293 ACC does not improve for 20 epochs. All experiments are conducted on hardware equipped with an
 294 NVIDIA GeForce RTX 4080 SUPER GPU.

295 **Evaluation Metrics** For the ID classification task, we use classification accuracy (ID ACC) as the
 296 evaluation metric. For the OOD detection task, we employ three standard metrics Wu et al. (2023):
 297 the area under the ROC curve (AUROC), the precision-recall curve (AUPR), and the false positive rate
 298 when the true positive rate reaches 95% (FPR@95). In all experiments, OOD nodes are considered
 299 positive cases. Detailed descriptions of these metrics are provided in Appendix C.

4.2 MAIN RESULTS

300 Table 1 presents the performance of various OOD detection methods across four datasets. From the
 301 results, we make several key observations:

302 **Effectiveness of LLM-driven OOD Exposure.** Both variants of GOE-LLM —GOE-identifier
 303 and GOE-generator—consistently outperform all methods that do not utilize OOD exposure. For
 304 example, on the Pubmed dataset, GOE-identifier achieves an AUROC of 0.8985, significantly
 305 surpassing GRASP (0.6627), the best-performing method without OOD exposure, resulting in a
 306 relative improvement of over 23.5%. This demonstrates that the pseudo-OOD nodes identified by the
 307 LLM provide meaningful supervision for learning precise decision boundaries in open-world settings.
 308 However, the improvement on the Wiki-CS dataset is much smaller, suggesting that the effectiveness
 309 of pseudo-OOD exposure depends on the dataset’s inherent difficulty and the extent of distributional
 310 shift. Due to space constraints, the standard deviation results are provided in Appendix D.

311 **Comparable Performance to Real OOD Supervision.** Remarkably, GOE-LLM achieves perfor-
 312 mance comparable to OE and GNNSafe++, both of which use real OOD nodes annotated by humans.
 313 On the Pubmed dataset, GOE-LLM even surpasses OE and GNNSafe++ in terms of AUROC and
 314 AUPR, despite relying solely on noisy pseudo-OOD nodes. This demonstrates that LLMs can serve
 315 as a practical alternative to costly OOD data curation. We attribute this strong performance to the
 316 LLM’s ability to synthesize semantically coherent yet distributionally distinct samples that effectively
 317 emulate the characteristics of true OOD data.

318 **ID Classification is Maintained.** A common concern with OOD exposure is its potential to degrade
 319 ID classification performance due to over-regularization. However, our results show that GOE-
 320 LLM maintains strong ID classification accuracy across all datasets. For example, on Citeseer,
 321 GOE-generator reaches 0.8552 ID accuracy, outperforming all other baselines. This indicates that
 322 pseudo-OOD nodes do not dilute the model’s ability to learn discriminative features for the ID task.

323 **Insights on LLM Annotations.** Although the OOD nodes identified by LLMs are relatively noisy (as
 324 shown in Section 4.4), using these noisy nodes to regularize the training of the ID classifier still yields

324
 325 Table 1: Performance comparison (best in **bold**, second-best in underline) of different methods on ID
 326 classification and OOD detection tasks. GOE-LLM achieves comparable performance to methods
 327 using real OOD nodes, while requiring no real OOD data and significantly outperforming methods
 328 without OOD exposure.

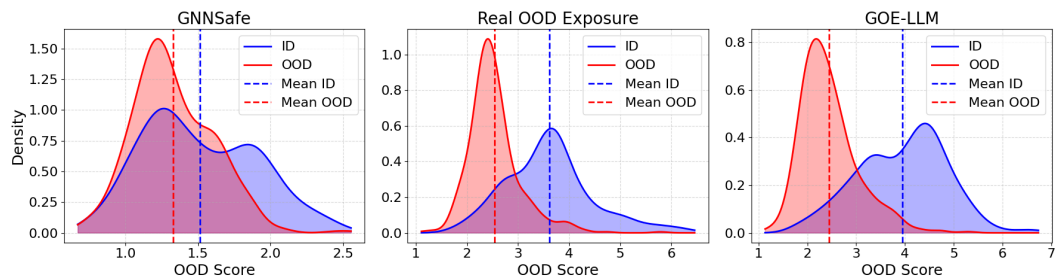
328 329 Model	330 Methods	331 Cora				332 Citeseer				333 Pubmed				334 Wiki-CS			
		335 ID ACC	336 AUROC	337 AUPR	338 FPR95	339 ID ACC	340 AUROC	341 AUPR	342 FPR95	343 ID ACC	344 AUROC	345 AUPR	346 FPR95	347 ID ACC	348 AUROC	349 AUPR	350 FPR95
	MSP	0.8748	0.8414	0.8506	0.6428	0.8480	0.7466	0.7500	0.7976	0.8776	0.6591	0.6623	0.8908	0.8648	0.7772	0.7851	0.7440
	Entropy	<u>0.8800</u>	0.8471	0.8549	0.6300	0.8480	0.7655	0.7603	0.7244	0.8776	0.6591	0.6623	0.8908	0.8640	0.7823	0.7891	0.7440
331 No OOD Exposure	Energy	0.8788	0.8580	0.8648	0.5928	<u>0.8504</u>	0.7757	0.7754	0.7256	0.8876	0.5861	0.5919	0.9296	0.8648	0.7983	0.8056	0.7320
332 GNNSafe	<u>0.8800</u>	0.9073	0.9073	0.4084	<u>0.8504</u>	0.7654	0.7697	0.8004	0.8916	0.5954	0.6403	0.8928	0.8752	0.8915	0.9144	0.7928	
333 GRASP	<u>0.8800</u>	0.9111	0.9034	0.3820	0.8460	0.7329	0.7429	0.8560	<u>0.8908</u>	0.6627	0.6956	0.8780	0.8768	0.8674	0.8864	0.7860	
334 Ours	GOE-identifier	0.8780	0.9264	0.9233	0.3268	0.8444	0.8107	0.8082	0.7104	0.8636	0.8985	0.8955	0.5108	0.8764	0.9014	0.9212	0.7728
335 Real OOD OE Exposure	GOE-generator	0.8792	0.9221	0.9208	0.3372	0.8552	0.7956	0.7994	0.7328	0.8820	0.7908	0.8035	0.7780	0.8752	0.9002	<u>0.9214</u>	<u>0.7288</u>
336 GNNSafe++		0.8792	<u>0.9371</u>	<u>0.9347</u>	<u>0.2944</u>	0.8464	<u>0.8180</u>	<u>0.8157</u>	<u>0.6832</u>	0.8760	<u>0.8852</u>	<u>0.8857</u>	<u>0.5568</u>	<u>0.8816</u>	<u>0.9048</u>	0.9254	0.7668

337 results on par with those obtained using real OOD nodes. The key intuition is that, while LLM-based
 338 annotations may be noisy, they are not arbitrary. In fact, they reflect a distributionally-aware semantic
 339 prior: nodes misclassified as OOD by the LLM often lie near the ID-OOD boundary and can serve
 340 as hard negatives. This is evident in our results, where even imprecise OOD exposure improves
 341 downstream detection performance significantly. This supports the hypothesis that OOD exposure
 342 does not need to be perfect to be effective—it merely needs to be informative enough to delineate
 343 boundaries in the feature space.

344 **Overall Impact.** Taken together, our findings suggest that LLM-driven pseudo-OOD exposure is a
 345 promising and scalable direction for graph OOD detection. It enables label-free OOD supervision,
 346 maintains strong ID classification, and yields competitive or superior results compared to both
 347 non-exposure and real-exposure methods.

348 4.3 IS THE CURRENT GRAPH OOD DETECTION SETTING PRACTICAL?

349 Since there is no established graph-specific OOD detection benchmark that models real distributional
 350 shifts among nodes, most existing work on node-level graph OOD detection simply assumes that
 351 nodes from randomly selected classes are designated as OOD. However, this setting has notable
 352 limitations. For example, if the ID classes are more heterogeneous or closely resemble the OOD
 353 classes, the ID classifier may fail to learn a well-defined decision boundary, resulting in high softmax
 354 confidence scores for OOD nodes. Additionally, if the set of ID classes spans a broad and diverse
 355 range of features, the model may naturally assign high confidence to OOD nodes, violating the
 356 common assumption that OOD nodes should receive lower confidence scores. Therefore, using real
 357 or pseudo-OOD nodes can provide a more realistic and effective training signal for OOD detection.
 358 By explicitly exposing the model to samples that are semantically or structurally different from the
 359 ID distribution, we can help the classifier better distinguish between ID and OOD nodes. This leads
 360 to more calibrated confidence estimates and improved robustness under open-world scenarios.



371 Figure 3: OOD score distributions of GNNSafe, GNNSafe++, and GOE-LLM on the Pubmed dataset.
 372 GOE-LLM, despite not using any real OOD nodes, achieves distributional separation comparable to
 373 the real OOD exposure method and significantly better separability than GNNSafe.

374 To demonstrate this, we visualize the OOD scores on the Pubmed dataset for GNNSafe, GOE-LLM,
 375 and GNNSafe++. As shown in Fig. 3, compared to the method without OOD exposure, our approach
 376 assigns notably lower OOD scores to ID nodes and higher scores to OOD nodes, resulting in a more
 377 distinct separation between the two groups.

378 4.4 ZERO-SHOT OOD ANNOTATION
379

380 We present the zero-shot OOD detection performance of the LLM. The prompt used for zero-shot
381 OOD node identification is provided in Prompt 4.4. For each dataset, we prompt the LLM to
382 determine whether each node in the test set (comprising 500 ID nodes and 500 OOD nodes) belongs
383 to one of the predefined ID categories; if not, the node is considered an OOD instance. We then
384 obtain binary OOD predictions from the LLM and compute its accuracy. The results are reported
385 in Table 2. We use accuracy as the sole evaluation metric for the LLM’s zero-shot OOD annotation
386 performance, since the LLM does not produce soft OOD scores (e.g., as defined in Eqn. 2), but rather
387 outputs hard binary decisions (0 or 1).

388 **PROMPT: Zero-Shot OOD Node Identification**
389

390 As a research scientist, your task is to analyze and classify {object} based on their
391 main topics, meanings, background, and methods.

392 Please first read the content of the {object} carefully. Then, identify the {object}’s
393 key focus. Finally, match the content to one of the given categories:

394 [Category 1, Category 2, Category 3, ...]

395 Given the current possible categories, determine if it belongs to one of them. If so,
396 specify that category; otherwise, say "none".

397 [Insert {Object} Content Here]

	Cora	Citeseer	Pubmed	Wiki-CS
Zero-shot OOD annotation	0.7190	0.7260	0.8410	0.7470

400 Table 2: Accuracy of using the LLM to identify whether unlabeled nodes are OOD. Although the
401 LLM-identified pseudo-OOD nodes are noisy, they still enable effective OOD exposure.

402 4.5 SYNTHETIC DATA MODEL
403

404 In this section, we combine labeled ID nodes and pseudo-OOD nodes to train the synthetic data
405 models, as described in Section 3.5. Specifically, we randomly select $20 \times K$ ID nodes and pseudo-
406 OOD nodes annotated by the LLM. In this way, we use the same number of ID and OOD nodes to
407 train the synthetic data models.

408 Table 3: Performance comparison (best highlighted in bold) of different synthetic data models on ID
409 classification and OOD detection tasks.

410 Methods	Cora				Citeseer				Pubmed				Wiki-CS			
	411 ACC ↑ AUROC ↑ AUPR ↑ FPR95 ↓	412 ACC ↑ AUROC ↑ AUPR ↑ FPR95 ↓	413 ACC ↑ AUROC ↑ AUPR ↑ FPR95 ↓	414 ACC ↑ AUROC ↑ AUPR ↑ FPR95 ↓	415 ACC ↑ AUROC ↑ AUPR ↑ FPR95 ↓	416 ACC ↑ AUROC ↑ AUPR ↑ FPR95 ↓	417 ACC ↑ AUROC ↑ AUPR ↑ FPR95 ↓	418 ACC ↑ AUROC ↑ AUPR ↑ FPR95 ↓	419 ACC ↑ AUROC ↑ AUPR ↑ FPR95 ↓	420 ACC ↑ AUROC ↑ AUPR ↑ FPR95 ↓	421 ACC ↑ AUROC ↑ AUPR ↑ FPR95 ↓	422 ACC ↑ AUROC ↑ AUPR ↑ FPR95 ↓	423 ACC ↑ AUROC ↑ AUPR ↑ FPR95 ↓	424 ACC ↑ AUROC ↑ AUPR ↑ FPR95 ↓	425 ACC ↑ AUROC ↑ AUPR ↑ FPR95 ↓	
GOE-LLM	0.8780	0.9264	0.9233	0.3268	0.8444	0.8107	0.8082	0.7104	0.8636	0.8985	0.8955	0.5108	0.8764	0.9014	0.9212	0.7728
($K + 1$)-Classifier	0.8716	0.9138	0.9185	0.4224	0.8336	0.8189	0.8200	0.6648	0.8840	0.9060	0.8968	0.3980	0.8684	0.8015	0.7923	0.6648

426 For the first approach, we can add a binary classification layer on top of the output features of the
427 ID classifier to predict the OOD score $z_{\text{ood}} = \mathbf{w}^\top \phi(x)$, where $\mathbf{w} \in \mathbb{R}^h$, and x is the output of
428 the hidden layer from the GNN-based ID classifier. The OOD score of node v_i is then defined as
429 $S_{\text{ood}}(v_i) = \sigma(z_{\text{ood}})$, where $\sigma(\cdot)$ denotes the sigmoid function. In the second approach, we train a
430 ($K + 1$)-class classifier and define the softmax probability of the ($K + 1$)-th class as the OOD score.
431 However, the performance of the first approach is not satisfactory in the current setting; therefore, we
432 only report the results of the ($K + 1$)-class classifier. The results are presented in Table 3. From the
433 results, we observe that using Eqn. 3 to regularize the training of the ID classifier does not degrade ID
434 classification performance. At the same time, it significantly improves OOD detection performance
435 compared to the baselines without OOD exposure. Furthermore, the ($K + 1$)-class classifier generally
436 achieves performance comparable to that of the regularization method.

437 4.6 HOW MANY SYNTHETIC OOD NODES DO WE NEED?

438 In this section, we prompt the LLM to generate different numbers of pseudo-OOD nodes. The prompt
439 used for OOD node generation is provided in Appendix E. Table 4 presents the ID classification and
440 OOD detection performance on the Pubmed dataset (which contains 19,717 nodes) using different
441 numbers of generated pseudo-OOD nodes. From the results, we can see that using more pseudo-
442 OOD nodes improves OOD detection performance. When the number of generated OOD nodes

432	433	Number of Pseudo-OOD Nodes	ID ACC \uparrow	AUROC \uparrow	AUPR \uparrow	FPR@95 \downarrow
434	435	0	0.8916	0.5954	0.6403	0.8928
436	437	2	0.8864	0.6692	0.6961	0.8708
438	439	3	0.8896	0.7401	0.7566	0.8100
440	441	5	0.8796	0.7674	0.7857	0.8036
442	443	10	0.8820	0.7908	0.8035	0.7780
444	445	20	0.8856	0.8043	0.8073	0.7400

439 reaches around 10, the performance nearly converges to a value that is significantly higher than that
440 achieved without OOD exposure. This suggests that even a small number of pseudo-OOD nodes can
441 provide meaningful OOD exposure during training, helping the model learn a more accurate decision
442 boundary between ID and OOD nodes. Moreover, it shows that LLM-generated pseudo-OOD nodes
443 offer an efficient and lightweight substitute for real OOD data. Another observation is that, among
444 all cases, the ID classification accuracy is highest when no OOD exposure is performed. However,
445 the degradation in ID classification performance is negligible when pseudo-OOD nodes are used to
446 regularize the training of the ID classifier. This further demonstrates that the trade-off described in
447 Section 3.2 is favorable, as pseudo-OOD exposure significantly improves OOD detection performance
448 while having minimal impact on ID classification accuracy.

449 450 4.7 COMPARISON ACROSS LLM VARIANTS

451 We experiment with the open-source model DeepSeek-V3 and the older LLM GPT-3.5-Turbo. The
452 results in Table 5 show only mild performance degradation with GPT-3.5 compared to GPT-4o-mini.
453 Moreover, using open-source LLMs for OOD node identification and generation yields comparable
454 detection performance, demonstrating that our approach is robust and reproducible with open-source
455 alternatives. The cost of querying the LLM for OOD annotations is reported in Appendix F.

456	457	Method	Cora				Citeseer			
			ID ACC \uparrow	AUROC \uparrow	AUPR \uparrow	FPR95 \downarrow	ID ACC \uparrow	AUROC \uparrow	AUPR \uparrow	FPR95 \downarrow
458	459	GOE-identifier (DeepSeek-V3)	0.8812	0.9288	0.9256	0.3136	0.8520	0.7902	0.7873	0.7612
460	461	GOE-generator (DeepSeek-V3)	0.8796	0.9244	0.9224	0.3252	0.8476	0.7815	0.7889	0.7696
462	463	GOE-identifier (GPT-3.5-Turbo)	0.8836	0.9202	0.9187	0.3340	0.8512	0.7978	0.7946	0.7488
464	465	GOE-generator (GPT-3.5-Turbo)	0.8796	0.9185	0.9173	0.3384	0.8512	0.7923	0.7978	0.7648

466 Table 5: Performance comparison of GOE-LLM with different LLMs on Cora and Citeseer datasets.

467 468 5 CONCLUSION

469 In this paper, we propose GOE-LLM, a novel framework for OOD detection on TAGs that eliminates
470 the reliance on real OOD data for exposure by leveraging LLMs. By designing two exposure
471 strategies—LLM-based OOD node identification and OOD node generation—we enable label-
472 efficient, scalable, and effective OOD exposure. Extensive experiments across diverse datasets
473 demonstrate that GOE-LLM achieves strong performance compared to methods relying on real
474 OOD data, and significantly surpasses existing methods without OOD exposure. Future work
475 could explore more advanced prompting strategies to improve the quality of pseudo-OOD samples.
476 Additionally, incorporating adaptive graph structure learning tailored to generated nodes may further
477 boost performance. Extending GOE-LLM to other graph learning tasks—such as graph-level OOD
478 detection and OOD detection on dynamic TAGs—also presents a promising direction.

479 **Broader Impact.** On the positive side, this work provides a practical and generalizable solution
480 to improve model reliability and robustness in open-world scenarios where labeled data is scarce
481 or dynamic changes are frequent. This has the potential to enhance safety and trustworthiness in
482 real-world deployments. On the other hand, our reliance on LLM-generated supervision introduces
483 challenges around semantic validity and bias. The quality and fairness of the pseudo-OOD labels
484 depend on the pretrained LLMs, which may inherit societal or domain-specific biases.

485 **Limitations.** First, the effectiveness of pseudo-OOD nodes relies on the LLM’s zero-shot accuracy;
486 inaccurate outputs may introduce noisy supervision. Second, while the proposed method markedly
487 improves OOD detection performance on many graph datasets, it is applicable only to TAGs. For
488 graphs without textual information, the method may be ineffective, highlighting the need for more
489 generalizable OOD exposure techniques. Further discussion is provided in Appendix H and I.

490 Table 4: Performance comparison using different numbers of generated pseudo-OOD
491 nodes for OOD exposure on the Pubmed
492 dataset. Even a small number of pseudo-
493 OOD nodes significantly improves OOD de-
494 tection performance.

486 ETHICS STATEMENT
487488 We adhere to the ICLR Code of Ethics and take full responsibility for this work. Our experiments
489 use public, de-identified text-attributed graph datasets (Cora, Citeseer, Pubmed, Wiki-CS) under
490 their licenses; no PII or new human-subject data were collected. LLMs were used only for pseudo-
491 OOD identification/generation and language editing, and all LLM-assisted text was reviewed by the
492 authors. We recognize potential misuse and mitigate it by releasing research-oriented code/prompts,
493 documenting limitations, and avoiding person-level datasets. To support fairness and transparency,
494 we report class splits, metrics, seeds, and ablations across datasets. Compute and environmental
495 impact are modest (small GNNs; limited training-time LLM calls; no LLMs at inference). Conflicts
496 of interest, if any, are disclosed per venue policy.
497498 REPRODUCIBILITY STATEMENT
499500 We provide complete details to facilitate replication. The formal description of our methods (GOE-
501 identifier, GOE-generator) and training procedures appears in Section 3 and Section 4, including
502 datasets, class partitions, and evaluation protocol. Dataset choices (Cora, Citeseer, Pubmed, Wiki-
503 CS) and ID/OOD class splits are described in the Experimental Setup and appendices. We specify
504 training/validation/test splits and report averages over five random seeds. Baselines and comparison
505 settings are enumerated alongside our methods to ensure parity. Prompts used for LLM-based
506 pseudo-OOD identification and generation are included in Section 4.4 and the appendix for exact
507 reuse. Additional ablations (e.g., varying the number of pseudo-OOD nodes) and efficiency analyses
508 are provided in the appendices. Our anonymous code repository is linked in the main paper for
509 end-to-end reproduction (data preprocessing, training scripts, and evaluation).
510511 REFERENCES
512513 Momin Abbas, Muneeza Azmat, Raya Horesh, and Mikhail Yurochkin. Out-of-distribution detection
514 using synthetic data generation. *arXiv preprint arXiv:2502.03323*, 2025.
515 Chentao Cao, Zhun Zhong, Zhanke Zhou, Yang Liu, Tongliang Liu, and Bo Han. Envisioning
516 outlier exposure by large language models for out-of-distribution detection. *arXiv preprint*
517 *arXiv:2406.00806*, 2024.
518 Hao Dong, Yue Zhao, Eleni Chatzi, and Olga Fink. Multiod: Scaling out-of-distribution detection
519 for multiple modalities. *Advances in Neural Information Processing Systems*, 37, 2024.
520 Xuefeng Du, Zhaoning Wang, Mu Cai, and Yixuan Li. Vos: Learning what you don't know by virtual
521 outlier synthesis. *arXiv preprint arXiv:2202.01197*, 2022.
522 Xuefeng Du, Zhen Fang, Ilias Diakonikolas, and Yixuan Li. How does unlabeled data provably help
523 out-of-distribution detection? *arXiv preprint arXiv:2402.03502*, 2024.
524 C Lee Giles, Kurt D Bollacker, and Steve Lawrence. Citeseer: An automatic citation indexing system.
525 In *Proceedings of the third ACM conference on Digital libraries*, pp. 89–98, 1998.
526 Dan Hendrycks and Kevin Gimpel. A baseline for detecting misclassified and out-of-distribution
527 examples in neural networks. *arXiv preprint arXiv:1610.02136*, 2016.
528 Dan Hendrycks, Mantas Mazeika, and Thomas Dietterich. Deep anomaly detection with outlier
529 exposure. *arXiv preprint arXiv:1812.04606*, 2018.
530 Dan Hendrycks, Andy Zou, Mantas Mazeika, Leonard Tang, Bo Li, Dawn Song, and Jacob Steinhardt.
531 Pixmix: Dreamlike pictures comprehensively improve safety measures. In *Proceedings of the*
532 *IEEE/CVF Conference on Computer Vision and Pattern Recognition*, pp. 16783–16792, 2022.
533 Nathan A Inkawich, Eric K Davis, Matthew J Inkawich, Uttam K Majumder, and Yiran Chen.
534 Training sar-atr models for reliable operation in open-world environments. *IEEE Journal of*
535 *Selected Topics in Applied Earth Observations and Remote Sensing*, 14:3954–3966, 2021.
536

540 Meng-Chieh Lee, Yue Zhao, Aluna Wang, Pierre Jinghong Liang, Leman Akoglu, Vincent S Tseng,
 541 and Christos Faloutsos. Autoaudit: Mining accounting and time-evolving graphs. In *2020 IEEE*
 542 *International Conference on Big Data (Big Data)*, pp. 950–956. IEEE, 2020.

543

544 Shawn Li, Huixian Gong, Hao Dong, Tiansai Yang, Zhengzhong Tu, and Yue Zhao. Dpu: Dynamic
 545 prototype updating for multimodal out-of-distribution detection. In *Proceedings of the IEEE/CVF*
 546 *Conference on Computer Vision and Pattern Recognition (CVPR)*, 2025.

547

548 Weitang Liu, Xiaoyun Wang, John Owens, and Yixuan Li. Energy-based out-of-distribution detection.
 549 *Advances in neural information processing systems*, 33:21464–21475, 2020.

549

550 Longfei Ma, Yiyu Sun, Kaize Ding, Zemin Liu, and Fei Wu. Revisiting score propagation in graph
 551 out-of-distribution detection. In *The Thirty-eighth Annual Conference on Neural Information*
 552 *Processing Systems*.

553

554 Andrew Kachites McCallum, Kamal Nigam, Jason Rennie, and Kristie Seymore. Automating the
 554 construction of internet portals with machine learning. *Information Retrieval*, 3:127–163, 2000.

555

556 Péter Mernyei and Cătălina Cangea. Wiki-cs: A wikipedia-based benchmark for graph neural
 557 networks. *arXiv preprint arXiv:2007.02901*, 2020.

558

559 Aristotelis-Angelos Papadopoulos, Mohammad Reza Rajati, Nazim Shaikh, and Jiamian Wang.
 560 Outlier exposure with confidence control for out-of-distribution detection. *Neurocomputing*, 441:
 138–150, 2021.

561

562 Yuehan Qin, Yichi Zhang, Yi Nian, Xueying Ding, and Yue Zhao. Metaood: Automatic selection of
 563 ood detection models. In *International Conference on Learning Representations (ICLR)*, 2025.

564

565 N Reimers. Sentence-bert: Sentence embeddings using siamese bert-networks. *arXiv preprint*
 566 *arXiv:1908.10084*, 2019.

566

567 Prithviraj Sen, Galileo Namata, Mustafa Bilgic, Lise Getoor, Brian Galligher, and Tina Eliassi-Rad.
 568 Collective classification in network data. *AI magazine*, 29(3):93–93, 2008.

569

570 Yu Song and Donglin Wang. Learning on graphs with out-of-distribution nodes. In *Proceedings of*
 571 *the 28th ACM SIGKDD Conference on Knowledge Discovery and Data Mining*, pp. 1635–1645,
 572 2022.

572

573 Leitian Tao, Xuefeng Du, Xiaojin Zhu, and Yixuan Li. Non-parametric outlier synthesis. *arXiv*
 574 *preprint arXiv:2303.02966*, 2023.

575

576 Sachin Vernekar, Ashish Gaurav, Vahdat Abdelzad, Taylor Denouden, Rick Salay, and Krzysztof Czar-
 577 necki. Out-of-distribution detection in classifiers via generation. *arXiv preprint arXiv:1910.04241*,
 578 2019.

578

579 Danny Wang, Ruihong Qiu, Guangdong Bai, and Zi Huang. Gold: Graph out-of-distribution detection
 580 via implicit adversarial latent generation. *arXiv preprint arXiv:2502.05780*, 2025.

581

582 Ziyu Wang, Bin Dai, David Wipf, and Jun Zhu. Further analysis of outlier detection with deep
 583 generative models. *Advances in Neural Information Processing Systems*, 33:8982–8992, 2020.

583

584 Qitian Wu, Yiting Chen, Chenxiao Yang, and Junchi Yan. Energy-based out-of-distribution detection
 585 for graph neural networks. *arXiv preprint arXiv:2302.02914*, 2023.

586

587 Zhiping Xiao, Weiping Song, Haoyan Xu, Zhicheng Ren, and Yizhou Sun. Timme: Twitter ideology-
 588 detection via multi-task multi-relational embedding. In *Proceedings of the 26th ACM SIGKDD*
 589 *international conference on knowledge discovery & data mining*, pp. 2258–2268, 2020.

589

590 Haoyan Xu, Runjian Chen, Yueyang Wang, Ziheng Duan, and Jie Feng. Cosimgnn: towards
 591 large-scale graph similarity computation. *arXiv preprint arXiv:2005.07115*, 2020.

592

593 Haoyan Xu, Ziheng Duan, Yueyang Wang, Jie Feng, Runjian Chen, Qianru Zhang, and Zhongbin
 593 Xu. Graph partitioning and graph neural network based hierarchical graph matching for graph
 594 similarity computation. *Neurocomputing*, 439:348–362, 2021.

594 Haoyan Xu, Kay Liu, Zhengtao Yao, Philip S Yu, Kaize Ding, and Yue Zhao. Lego-learn: Label-
 595 efficient graph open-set learning. *Transactions on Machine Learning Research*, 2025a.
 596

597 Haoyan Xu, Zhengtao Yao, Yushun Dong, Ziyi Wang, Ryan A Rossi, Mengyuan Li, and Yue Zhao.
 598 Few-shot graph out-of-distribution detection with llms. *arXiv preprint arXiv:2503.22097*, 2025b.

599 Hao Yan, Chaozhuo Li, Ruosong Long, Chao Yan, Jianan Zhao, Wenwen Zhuang, Jun Yin, Peiyan
 600 Zhang, Weihao Han, Hao Sun, et al. A comprehensive study on text-attributed graphs: Bench-
 601 marking and rethinking. *Advances in Neural Information Processing Systems*, 36:17238–17264,
 602 2023.

603 Jingkang Yang, Kaiyang Zhou, Yixuan Li, and Ziwei Liu. Generalized out-of-distribution detection:
 604 A survey. *International Journal of Computer Vision*, 132(12):5635–5662, 2024.

605

606 Junhan Yang, Zheng Liu, Shitao Xiao, Chaozhuo Li, Defu Lian, Sanjay Agrawal, Amit Singh,
 607 Guangzhong Sun, and Xing Xie. Graphformers: Gnn-nested transformers for representation
 608 learning on textual graph. *Advances in Neural Information Processing Systems*, 34:28798–28810,
 609 2021.

610 Jingyang Zhang, Nathan Inkawich, Randolph Linderman, Yiran Chen, and Hai Li. Mixture outlier
 611 exposure: Towards out-of-distribution detection in fine-grained environments. In *Proceedings of
 612 the IEEE/CVF Winter Conference on Applications of Computer Vision*, pp. 5531–5540, 2023.

613

614 Xujiang Zhao, Feng Chen, Shu Hu, and Jin-Hee Cho. Uncertainty aware semi-supervised learning on
 615 graph data. *Advances in neural information processing systems*, 33:12827–12836, 2020.

616

617 Yanqiao Zhu, Yuanqi Du, Yinkai Wang, Yichen Xu, Jieyu Zhang, Qiang Liu, and Shu Wu. A survey
 618 on deep graph generation: Methods and applications. In *Learning on Graphs Conference*, pp. 47–1.
 619 PMLR, 2022.

620

621

622

623

624

625

626

627

628

629

630

631

632

633

634

635

636

637

638

639

640

641

642

643

644

645

646

647

648 APPENDIX: GRAPH SYNTHETIC OUT-OF-DISTRIBUTION EXPOSURE WITH
 649 LARGE LANGUAGE MODELS
 650

651 A ID AND OOD SPLIT
 652
 653

654 Table 6: ID classes and ID ratio for different datasets.

655 Dataset	656 ID class	657 ID ratio
658 Cora	[2, 4, 5, 6]	47.71%
659 Citeseer	[0, 1, 2]	55.62%
660 WikiCS	[1, 4, 5, 6]	38.79%
661 Pubmed	[0, 1]	60.75%

662 B DATASET DESCRIPTIONS
 663

664 **Cora** The Cora dataset McCallum et al. (2000) contains 2,708 scientific publications categorized
 665 into seven research topics: case-based reasoning, genetic algorithms, neural networks, probabilistic
 666 methods, reinforcement learning, rule learning, and theory. Each node represents a paper, and edges
 667 correspond to citation links between papers, forming a graph with 5,429 edges.

668 **CiteSeer** The CiteSeer dataset Giles et al. (1998) consists of 3,186 scientific articles classified
 669 into six research domains: Agents, Machine Learning, Information Retrieval, Databases, Human-
 670 Computer Interaction, and Artificial Intelligence. Each node represents a paper, with node features
 671 extracted from the paper’s title and abstract. The graph is constructed based on citation relationships
 672 among the publications.

673 **WikiCS** WikiCS Mernyei & Cangea (2020) is a Wikipedia-based graph dataset constructed for
 674 benchmarking graph neural networks. Nodes correspond to articles in computer science, divided into
 675 ten subfields serving as classification labels. Edges represent hyperlinks between articles, and node
 676 features are derived from the corresponding article texts.

677 **PubMed** The PubMed dataset Sen et al. (2008) comprises scientific articles related to diabetes
 678 research, divided into three categories: experimental studies on mechanisms and treatments, research
 679 on Type 1 Diabetes with an autoimmune focus, and Type 2 Diabetes studies emphasizing insulin
 680 resistance and management. The citation graph connects related papers, with node features derived
 681 from medical abstracts.

682 C EVALUATION METRICS
 683

684 We use the following metrics to evaluate in-distribution (ID) classification and out-of-distribution
 685 (OOD) detection performance, which are widely used OOD detection research Dong et al. (2024); Li
 686 et al. (2025); Qin et al. (2025):

687 **Accuracy (ACC)** Measures the proportion of correctly classified ID nodes:

$$688 \text{ACC} = \frac{1}{|\mathcal{D}_{\text{ID}}|} \sum_{x_i \in \mathcal{D}_{\text{ID}}} \mathbb{I}[\hat{y}_i = y_i], \quad (6)$$

690 where \hat{y}_i is the predicted class label and y_i is the true class label.

691 **Area Under the ROC Curve (AUROC)** Evaluates how well the OOD detector ranks OOD nodes
 692 higher than ID nodes based on their OOD scores. It is defined as:

$$693 \text{AUROC} = \mathbb{P}(s_{\text{OOD}}(x_{\text{OOD}}) > s_{\text{OOD}}(x_{\text{ID}})), \quad (7)$$

694 where $s_{\text{OOD}}(\cdot)$ denotes the OOD score function.

702 **Area Under the Precision-Recall Curve (AUPR)** Measures the area under the curve defined by
 703 precision and recall:
 704

$$705 \quad \text{Precision} = \frac{\text{TP}}{\text{TP} + \text{FP}}, \quad (8)$$

$$707 \quad \text{Recall} = \frac{\text{TP}}{\text{TP} + \text{FN}}, \quad (9)$$

$$709 \quad \text{AUPR} = \int_0^1 \text{Precision}(r) dr, \quad (10)$$

711 where OOD nodes are treated as the positive class, and r denotes recall.
 712

713 **False Positive Rate at 95% True Positive Rate (FPR@95)** Indicates the fraction of ID samples
 714 incorrectly predicted as OOD when the true positive rate (TPR) on OOD samples is 95%:
 715

$$716 \quad \text{FPR@95} = \left. \frac{\text{FP}_{\text{ID}}}{\text{FP}_{\text{ID}} + \text{TN}_{\text{ID}}} \right|_{\text{TPR}=0.95}, \quad (11)$$

718 where FP and TN are false positives and true negatives on ID data, respectively.
 719

720 D STANDARD DEVIATION RESULTS

724 Table 7: Standard deviation results for various models across ID classification and OOD detection
 725 metrics. All values are in percentages.

726 Model	727 Methods	728 Cora				729 Citeseer				730 Pubmed				731 Wiki-CS			
		732 ACC	733 AUROC	734 AUPR	735 FPR95	736 ACC	737 AUROC	738 AUPR	739 FPR95	740 ACC	741 AUROC	742 AUPR	743 FPR95	744 ACC	745 AUROC	746 AUPR	747 FPR95
748 No OOD 749 Exposure	MSP	2.46	1.90	1.47	7.68	1.39	2.85	3.04	5.38	3.06	2.12	3.02	2.37	2.73	3.65	4.19	6.74
	Entropy	2.18	2.78	1.87	8.91	1.39	2.59	2.80	6.31	3.06	2.12	3.02	2.37	2.71	3.33	3.71	7.10
	Energy	2.17	2.18	1.58	9.95	1.61	2.54	2.27	5.68	1.13	8.70	9.23	2.82	2.67	5.70	4.92	13.74
	GNNSafe	2.18	1.74	2.12	10.52	1.61	2.58	2.36	5.91	1.23	14.34	13.08	8.26	2.63	0.80	0.90	16.60
	GRASP	2.18	1.88	1.34	13.29	1.62	2.88	2.82	6.92	1.32	12.34	11.76	5.70	2.92	2.58	3.18	12.96
750 Ours	GOE-identifier	2.53	0.88	1.42	2.24	1.65	2.01	1.85	7.66	2.03	2.48	3.02	7.69	2.20	0.90	1.26	11.86
	GOE-generator	2.18	1.67	2.12	7.03	1.49	1.31	1.58	7.12	2.69	6.86	5.62	7.79	2.66	1.22	1.09	1.62
751 Real OOD 752 Exposure	OE	1.86	1.19	1.03	6.39	1.60	2.57	2.24	11.08	1.88	5.17	5.27	14.78	1.40	1.64	1.71	9.08
	GNNSafe++	2.57	0.93	1.46	3.84	1.47	2.08	2.22	8.69	1.26	3.83	3.45	1.13	2.41	1.04	1.32	12.27

739 E PROMPT FOR OOD NODE GENERATION

741 PROMPT: LLM-Based OOD Node Generation

743 Please generate {num_generated_samples} {object}(s) belonging to the
 744 category '{category_name}', including title and abstract.

745 Output Format:

- 746 • Title: <Generated Title>
- 747 • Abstract: <Generated Abstract>

750 F EFFICIENCY AND COST ANALYSIS.

753 During training, GOE-identifier involves approximately 200 LLM API calls per dataset for node
 754 annotation, each taking ~1 second per call. GOE-generator typically involves generating around 10
 755 synthetic nodes per OOD class, resulting in approximately 10–50 API calls per dataset, each call
 taking ~1 second.

756 However, our method is highly efficient at inference. Unlike directly using an LLM for OOD detection,
 757 it relies solely on the trained GNN-based ID classifier, yielding significantly faster inference. As
 758 shown in Table 8, no LLM components are involved, resulting in inference speeds comparable to
 759 post-hoc OOD detection methods.

760 The monetary cost of querying the LLM (GPT-4o-mini) for annotations is reported in Table 9. By
 761 default, GOE-identifier uses the LLM to **annotate 200 nodes** per dataset, while GOE-generator
 762 **generates** $10 \times K$ **nodes** per dataset. For example, on the Cora dataset, GOE-identifier costs **\$0.0236**
 763 in total, and GOE-generator costs **\$0.007** in total.

	GNNSafe	GOE-identifier	GOE-generator
Training time (s)	0.45	0.56	0.50
Inference time (s)	0.0023	0.0024	0.0024

770 Table 8: Training and inference times of GNNSafe, GOE-identifier, and GOE-generator on the
 771 Citeseer dataset.

	GOE-identifier	GOE-generator
Total cost	\$0.02357 / 200 nodes	\$0.00702 / 30 nodes
Cost per node	\$0.000118 / node	\$0.000234 / node

779 Table 9: Monetary cost of GOE-identifier and GOE-generator when using GPT-4o-mini for annotations
 780 on the Cora dataset.

783 G COMPARISON WITH ZERO-SHOT LLM DETECTION

785 In the following table, we also report the results of directly using binary OOD predictions from
 786 the LLM to compute OOD detection metrics (AUROC, AUPR, FPR95). This direct comparison
 787 demonstrates that our proposed synthetic OOD exposure strategy significantly improves OOD
 788 detection performance over zero-shot LLM detection alone.

Method	Cora				Citeseer			
	ID ACC \uparrow	AUROC \uparrow	AUPR \uparrow	FPR95 \downarrow	ID ACC \uparrow	AUROC \uparrow	AUPR \uparrow	FPR95 \downarrow
LLM-zero-shot	0.6032	0.7310	0.7982	1.0000	0.4400	0.7268	0.8087	1.0000
GOE-LLM	0.8780	0.9264	0.9233	0.3268	0.8444	0.8107	0.8082	0.7104

755 Table 10: Comparison of zero-shot LLM OOD detection versus GOE-LLM with synthetic OOD
 756 exposure on Cora and Citeseer datasets

800 H DISCUSSION ON POTENTIAL OVERLAP BETWEEN LLM TRAINING DATA 801 AND EVALUATION DATASETS.

803 GPT-4o-mini is a proprietary model, and detailed training corpus information is not publicly available.
 804 While we cannot rule out potential overlap entirely, commonly used graph datasets (Cora, Citeseer,
 805 PubMed, Wiki-CS) are likely represented to some extent in the LLM training corpus. However,
 806 since our method uses only class labels and general knowledge for OOD generation (rather than
 807 direct dataset memorization), we consider the impact of any possible overlap minimal. We further
 808 conduct experiments with additional LLMs (GPT-3.5-Turbo and DeepSeek-V3) and observe that
 809 pseudo-OOD annotations produced by these LLMs consistently lead to significant improvements in
 OOD detection performance.

810 I DISCUSSION ON SPECIALIZED DOMAIN APPLICABILITY
811812 In this paper, we primarily evaluate our method on widely used benchmarks. For specialized or less
813 common domains, our approach may require tailored LLM prompting strategies due to differences
814 in domain knowledge. For example, even in well-studied domains, if the ID classes are highly
815 heterogeneous or closely resemble the OOD classes, the ID classifier may fail to learn a clear decision
816 boundary, resulting in high softmax confidence scores for OOD nodes. In this scenario, training
817 the ID classifier solely on ID nodes (as most existing graph OOD detection methods do) leads to
818 poor performance. For instance, on the PubMed dataset, although baselines achieve accurate ID
819 classification, their OOD detection performance is nearly random. Our proposed method leverages
820 pseudo-OOD nodes to provide a more realistic and effective training signal, substantially enhancing
821 the ID classifier’s OOD awareness and improving performance by 23.5% over the best-performing
822 baseline. This result suggests that our method offers a greater advantage in OOD detection compared
823 to baselines, particularly in specialized domains such as complex scientific research (e.g., the PubMed
824 dataset). While our method is more effective than prior approaches, we recommend exploring
825 domain-specific adjustments in future work.
826827 J THE USE OF LARGE LANGUAGE MODELS (LLMs)
828829 In accordance with the conference policy on LLM usage, we disclose the role of LLMs in this work.
830 We used OpenAI’s ChatGPT both as part of our methodology and as a writing assistant. Methodolog-
831 ically, it was employed for (1) pseudo-OOD node identification, where the LLM classified sampled
832 unlabeled nodes as ID or OOD in a zero-shot setting, and (2) pseudo-OOD node generation, where
833 the LLM produced synthetic OOD node texts. For writing, it assisted with (3) improving clarity,
834 conciseness, and grammar of drafts, (4) suggesting alternative phrasings for technical descriptions,
835 and (5) LaTeX table and figure formatting.
836837 LLMs were not involved in research ideation, experimental design, or result interpretation. All
838 scientific contributions, including problem conception, method development, experimental setup,
839 and analysis, were conducted by the authors. The authors carefully reviewed and verified all LLM
840 outputs (including generated nodes) to ensure accuracy, appropriateness, and originality, and take full
841 responsibility for the final content. LLMs are not considered contributors or authors.
842
843
844
845
846
847
848
849
850
851
852
853
854
855
856
857
858
859
860
861
862
863

864
865
866
867
868
869
870
871
872
873
874
875
876
877
878
879
880
881
882
883
884
885
886
887
888
889
890
891
892
893
894
895
896
897
898
899
900
901
902
903
904
905
906
907
908
909
910
911
912
913
914
915
916
917
K OOD DETECTION METHODS COMPARISON

Method	Core Technique	Uses LLM?	LLM Role (if any)	Requires Real OOD Data?	Data Type
GNNSafe Wu et al. (2023)	Post-hoc Energy Scoring	No	N/A	No	Graph
GRASP Ma et al.	Post-hoc Score Propagation	No	N/A	No	Graph
GNNSafe++ Wu et al. (2023)	OOD Exposure (Real Data) + Energy Regularization	No	N/A	Yes	Graph
VOS Du et al. (2022)	Generative Pseudo-OOD (Representations)	No	N/A	No	Image
GOLD Wang et al. (2025)	Implicit Adversarial Pseudo-OOD Latent Generation	No	N/A	No	Graph
Synthetic Abbas et al. (2025)	LLM-Generated Pseudo-OOD Proxies	Yes	Pseudo-OOD Text Generation	No	Text
EOE Cao et al. (2024)	LLM-Envisioned Outlier Exposure	Yes	Outlier Concept Generation	No	Image
GOE-identifier	OOD Exposure (LLM-Identified Pseudo-OOD Nodes)	Yes	Pseudo-OOD Node Identification	No	Text-Attributed Graph
GOE-generator	OOD Exposure (LLM-Generated Pseudo-OOD Nodes)	Yes	Pseudo-OOD Node Generation	No	Text-Attributed Graph

Table 11: Comparison of various OOD detection methods.